

TITLE

Experimental method to determine specific heat and transition enthalpy at a first-order phase transition: fundamentals and application to a NiMnIn Heusler alloy

F. J. Romero (fjromero@us.es), M.C. Gallardo (mcgallar@us.es), J.M. Martín-Olalla (olalla@us.es), J. del Cerro (delcerro@us.es).

Departamento de Física de la Materia Condensada. Facultad de Física. Universidad de Sevilla.
Avenida Reina Mercedes s/n 41012 Sevilla SPAIN

Corresponding author: F.J. Romero (fjromero@us.es)

ABSTRACT

A new method that characterizes thermal properties during a first-order phase transition is described. The technique consists in exciting the sample by a series of constant frequency thermal pulses which one in every N pulses -- N is a small number like four—being exceedingly large in amplitude. This pulse induces phase transformation which is inhibited during the following smaller pulses due to thermal hysteresis. That way the specific heat for a given mixture of phases can be determined. The results obtained are independent of experimental parameters like the rate and the amplitude of the pulses, unlike what happens in other calorimetric techniques. The method also provides the enthalpy excess by analysing the energy balance between the dissipated heat and the heat flowing during each pulse of measurement.

The protocol is tested to analyse the phase transitions of a Heusler alloy $\text{Ni}_{50.54}\text{Mn}_{33.65}\text{In}_{15.82}$. The paramagnetic-ferromagnetic transition for the austenite phase is continuous and the specific heat shows a lambda anomaly. The martensitic phase transition shows a first-order character and the specific heat follows a step-like behaviour in contrast with previously reported large-peak anomalies.

Keywords: specific heat, latent heat, enthalpy, phase transition, Heusler alloy

1. INTRODUCTION

The measure of thermal properties such as specific heat, enthalpy and entropy is paramount in many topics of physics, chemistry or materials science [1] like the characterization of phase transitions. Thermal properties integrate every contribution to the free energy of the system and thus provide a unique information of the system.

First-order phase transitions are characterized by a few defining properties. They ideally happen at a given temperature. Energy exchange does not cause the sample to heat or cool (sensible heat), instead it causes phase transformation (latent heat) altering the molar fraction of coexisting phases [2]. Thermal properties like entropy and enthalpy excesses show a discontinuity while the specific heat has a singularity at the transition point since the exchange of energy does not cause a change of temperature. An additional feature is the presence of thermal hysteresis between cooling and heating runs.

In real systems this sharp behaviour is usually smeared: temperature gradients, internal stresses, sample inhomogeneities, defects and the like make the transition to happen over an extended range of temperature. The latent heat spreads over that temperature interval and there is also a variation of the specific heat since some fraction of the sample is modifying its temperature.

As a result of all this, the measure of thermal properties during a first-order phase transition is always challenging.

Different techniques such as adiabatic calorimetry [3], ac calorimetry [4], differential thermal analysis and differential scanning calorimetry [1], relaxation calorimetry [5] or conduction calorimetry [6] have been developed to measure thermal properties. In the simplest case specific heat is measured by exciting the sample with a thermal pulse which usually changes sample temperature and addenda temperature. The ratio of the pulse to the change of temperature evaluates the specific heat as per its raw definition.

First-order phase transitions challenge these methods since the experimentalist must discriminate which portion of the heat pulse caused phase transformation (latent heat) and which portion, if any at all, caused a change of temperature (sensible heat). When this is not possible specific heat data may not be reproducible because they could depend on the experimental setup including parameters like the amplitude of the heat pulses and the temperature variation rate. Previous studies have also focused on the ways of discriminating heat capacity data under these circumstances [7-11].

We previously developed a method called Squared Modulated Differential Thermal Analysis (SMDTA) which was able to characterize continuous (second-order) and discontinuous (first-order) phase transitions [12,13] even in the neighborhood of a tricritical point where the challenges grow because the specific heat is expected to diverge.

This paper introduces an improvement of the SMDTA technique that allows the measurement of the heat capacity during a first-order phase transition. Unlike the original method, the new technique employs amplitude-modulated thermal pulses, with one in every N pulses being exceedingly large. We take advantage of the thermal hysteresis that follows the large thermal pulse and which inhibits subsequent phase transformations. The fundamental of the method could be applied to other types of calorimetry. For testing the method we choose a Heusler type alloy ($\text{Ni}_{50.54}\text{Mn}_{33.65}\text{In}_{15.82}$) which exhibits a second-order para-ferromagnetic phase transition followed by a first-order martensitic phase transition [14].

2. EXPERIMENTAL

The sample was nearly octagonal with flat faces of area 90 mm^2 and 1.89mm height. The mass of the sample was 1.5487 g. Sample composition was determined as $\text{Ni}_{50.54}\text{Mn}_{33.65}\text{In}_{15.82}$ from energy dispersive X-ray fluorescence measurements (spectrometer EDAX $\mu\text{FRXEAGLE III}$) at the Research, Technology and Innovation Centre (CITIUS, University of Sevilla, Spain).

The experimental device has been described elsewhere [15]. The sample is sandwiched between two heat fluxmeters, rigid enough to support the sample and to apply, if necessary, a controlled uniaxial stress on the sample. The other end of each fluxmeter is in thermal contact with a calorimetric block. The thermal stability of the equipment allows modifying the temperature of the calorimetric block at rates of 0.02 K/h-0.30 K/h. Two heaters are placed between the sample and the fluxmeters, which can be used to supply heat pulses, whose effect is superposed to the temperature ramp. Heat pulses are able to achieve a temperature amplitude ranging from 0.01K to 0.25K.

3. METHOD

The specific heat of the sample is measured using the following procedure [6]. At time $t=t_0$ the heaters begin to supply a constant power W_0 for a time τ long enough to let the sample reach

a steady state temperature distribution, characterized by a temperature difference ΔT_1 between the sample and the calorimetric block. At time $t_1=t_0+\tau$, the power W_0 is cut off and the sample relaxes to a new steady state temperature distribution at time $t_2=t_0+2\tau$. The electromotive force given by the fluxmeters $V(t)$ is measured during the described process. $V(t)$ is proportional to the heat flux $\phi(t)$ crossing the fluxmeters, $\phi(t) = V(t)/\alpha$, where α is the sensitivity of the fluxmeters, determined by calibration.

Figure 1 shows an ideal square pulse and the transient response $V(t)$ by the fluxmeters. The integral of the heat flux over the duration of one cycle (grey area in Figure 1) amounts to the total energy supplied by the heaters $Q=W_0 \tau$.

$$\int_{t_0}^{t_0+2\tau} (\phi - \phi_0) dt = \int_{t_0}^{t_0+2\tau} \frac{V-V_0}{\alpha} dt = W_0 \tau = Q \quad (1)$$

Two normalized areas A_d and A_r corresponding to the dissipation and the relaxation branch respectively can be obtained as:

$$A_d = \tau - \int_{t_0}^{t_0+\tau} \frac{V-V_0}{V_1-V_0} dt \quad (2)$$

$$A_r = \int_{t_0+\tau}^{t_0+2\tau} \frac{V-V_0}{V_1-V_0} dt \quad (3)$$

In another experiment with no sample attached to the fluxmeters the calibrating normalized areas A_d^0 and A_r^0 are determined.

Specific heat data are obtained from [12]:

$$mc_d = \frac{2}{\beta} (A_d - A_d^0) \quad (4)$$

$$mc_r = \frac{2}{\beta} (A_r - A_r^0) \quad (5)$$

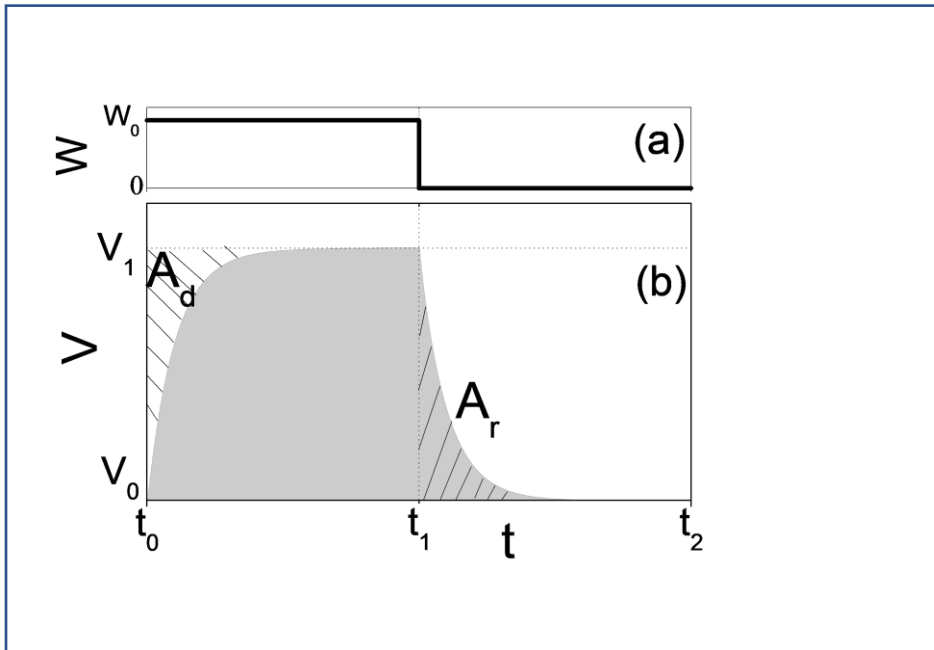


Figure 1: power dissipated $W(t)$ in the heaters (a) and transient response $V(t)$ given by the fluxmeters (b).

where m is the mass of the sample and β is the thermal resistance of the fluxmeters obtained by calibration. When no kinetic process is present, both branches results are equivalent.

Due to the large thermal inertia of the calorimetric block this protocol seldom operates in this equilibrium configuration. Instead it operates while the temperature of the calorimetric block is steadily varying at a low rate. Figure 2 shows (panel a and b) a series of thermal pulses and responses; panel (c) shows the evolution of sample temperature with time when the temperature of the calorimetric block is steadily increasing.

When the temperature of the sample reaches a first-order phase transition the thermal pulse will trigger the phase transformation into the high temperature phase. Now energy is not stored as an increase of temperature (sensible heat) but as a structural transformation (latent heat). This will modify the response of the fluxmeters [13,16] and Eqs. 4 and 5 from which specific heat is extracted do not hold.

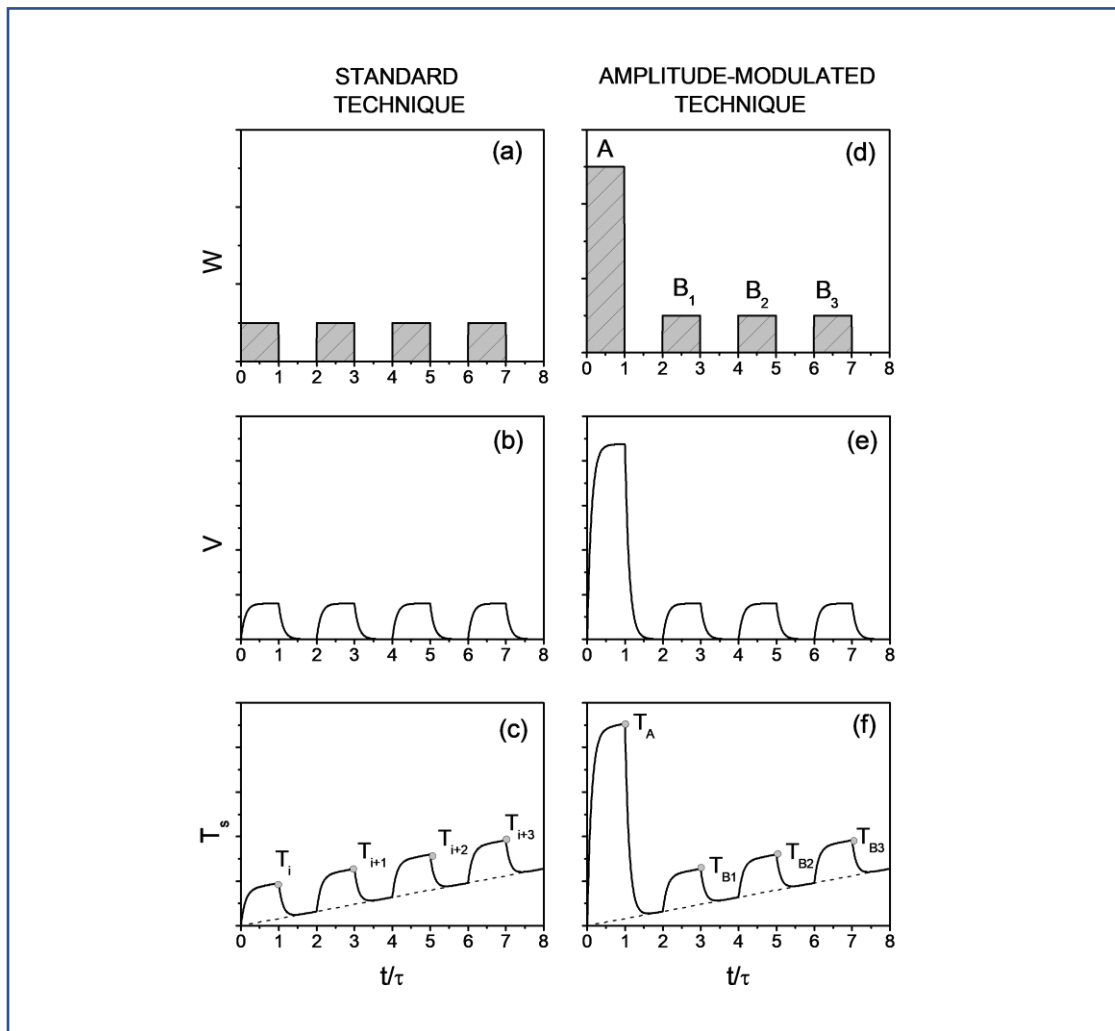


Figure 2: On the left, a train of square heat pulses with equal amplitude and period (a); the associated response in the fluxmeters (b); and change of temperature in the sample if a stationary rate of temperature change is set on the calorimetric block. On the right, a train of square heat pulses of equal period but with modulated amplitude, the first out of four pulses is exceedingly large amplitude (d); the associated fluxmeter signal (e) and the change of temperature in the sample (f).

Also in this case, the difference between the integral of the heat flux and Q is the enthalpy change exchanged in this cycle ΔH_i .

$$\Delta H_i = W_0 \tau - \int_{t_0}^{t_0 + 2\tau} (\phi - \phi_0) dt \quad (6)$$

Notice that in any of the cycles where the temperature of the sample is within the coexistence interval, the sample will be partially transformed to the high temperature phase since the temperature steadily increases with every cycle ($T_{i+1} > T_i$, see Figure 2c). This fact will happen irrespective of the temperature variation range or the applied heat power.

The new method we present in this work is based in a train of N pulses of which the first one (A) is exceedingly large than the remaining pulses (B), see Figure 2d. During a first-order phase transition pulse A will transform a fraction of the sample into the new high temperature phase but during the relaxation process thermal hysteresis will inhibit the backward transformation. Thereafter pulse B will not ideally induce new phase transformation since the temperature of sample does not exceed the maximum temperature reached during pulse A ($T_{Bi} < T_{Ai}$, see Figure 2f). The transformation resumes only when the following pulse A is onset.

In this scenario the enthalpy excess can be determined from the energetic balance of the cycles. On the other hand reproducible specific heat values can be obtained from Eq. 4 and 5 only for B-pulses. The normalized areas of pulses A are not related to specific heat since phase transformation occurs in these cases and fluxmeter responses are distorted [13,16] as energy is structurally stored.

These hypotheses will only be sound as long as the amplitude of pulse A, the amplitude of pulse B and the rate of change of temperature are appropriately set in the way that the temperature of the sample does not exceed maximum temperature reached on pulse A ($T_{Bi} < T_{Ai}$, see figure 2f). We recall that the phase transition takes place over an extended range of temperature due to internal stresses, inhomogeneities or defects, to name a few.

For each pulse, Equation (6) is computed. For the first pulse it is expected that $\Delta H_i \neq 0$ if the transition is first-order. If the parameters are set appropriately for the following $N-1$ pulses or when no phase transition is occurring $Q_i = \tau W_i$ and the integral should match to each other within the experimental resolution.

The transition enthalpy will be calculated from $\Delta H_i = \sum_i \Delta H_i$ and the coexistence interval will be obtained by analysing the temperatures at which the condition $\Delta H_i \neq 0$ has been fulfilled.

4. RESULTS AND DISCUSSION

According to the phase diagram of $\text{Ni}_{50}\text{Mn}_{50-x}\text{In}_x$ alloys [17], a sample of composition $\text{Ni}_{50.54}\text{Mn}_{33.65}\text{In}_{15.82}$ undergoes two phase transitions which are close to each other and near room temperature. On cooling there is a phase transition between paramagnetic-austenitic and ferromagnetic-austenitic phases followed by an austenitic-martensitic transition.

In a first run, we recorded the specific heat using the standard procedure [6,13] which consists of a series of identical square thermal pulses. The first run was performed under a temperature scanning rate $r=0.18$ K/h and the power dissipated ($W=0.58$ mW, $Q=0.84$ J) in the heaters was selected to produce a temperature increment $\Delta T=0.035$ K at the end of the dissipation branch. We measured the time constant (78 s) and selected $\tau=720$ s. A lambda-like

anomaly was observed around 310 K associated to the ferro-paramagnetic (FP) transition of the austenite phase. Despite the compositional variation, the signature is similar to the anomaly seen for other members of the same family [18,19]. At lower temperatures, a strong peak was observed around 288 K which is associated to the austenitic-martensitic (M) phase transition. Sharp peaks have been also observed for the martensitic transition of NiMnIn, NiMnInCo or NiMnInSn [14,18-22].

Except around the M transition c_d and c_r match to each other within experimental resolution. We have shown previously that a difference between c_d and c_r is an evidence of a first-order phase transition[12]. Martensitic phase transitions are known to show athermal behaviour, so that there is a distribution of transition temperatures and the latent heat spreads over a wide temperature interval. Scattering of c_d and c_r is likely to be due to the intermittent dynamic of the martensitic transformation which produces quasi-instantaneous heat flux peaks of different amplitudes and durations [23-27].

To shrink the fraction of sample that is transformed during each cycle we reduced the dissipated power ($W=0.15\text{mW}$, $Q=0.11\text{J}$, $\Delta T=0.01\text{K}$) as well as the temperature variation rate ($r=0.04\text{ K/h}$) in a second run. The results are also shown in Figure 3. Data for the first and second run coincide over all the temperature interval except for the martensitic phase transition. There is no influence of the measuring parameters on the second order phase transition around 310K. However, during the M transformation the second run produces an anomaly which is markedly lower and narrower than that observed in the first run. Interestingly c_d and c_r keep showing a noisy distribution.

Therefore, experimental conditions impact the results. We stress the fact that this is happening even when the temperature scan rate is as low as 0.04 K/h and the amplitude of the thermal pulse on the sample is as low as 0.01 K. The magnitude and the width of the peak depends on the experimental conditions that modify the kinetics of the transformation, even if the experimental device is not altered. Under different kinetics, the molar fraction of each

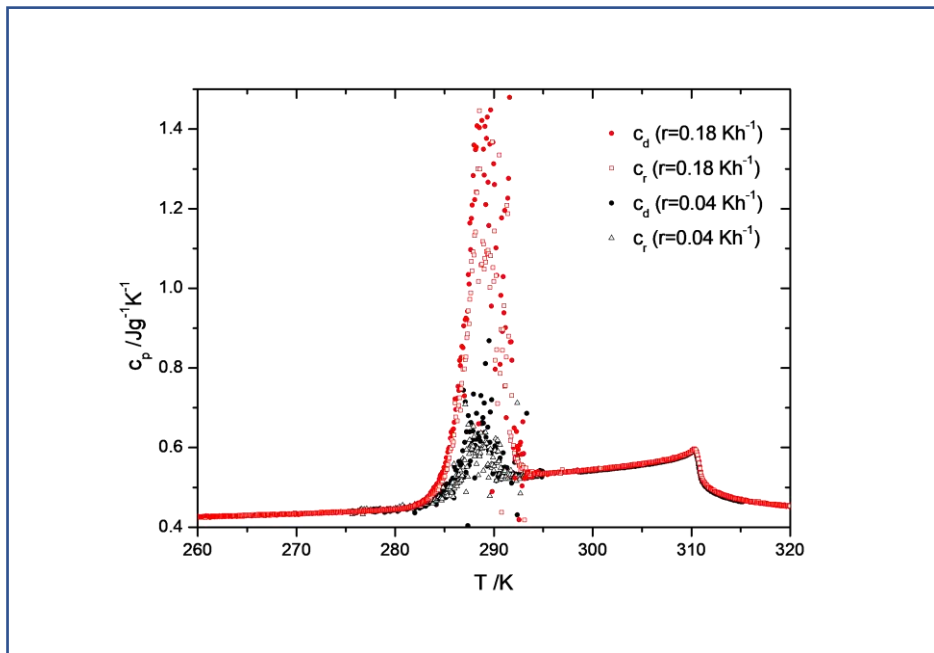


Figure 3: Specific heat data vs temperature in a $\text{Ni}_{50.54}\text{Mn}_{33.65}\text{In}_{15.82}$ sample. Specific heat data were obtained from Eq. 4 and 5 after a train of identical heat pulses excited the sample.

phase evolves in a different way and the results for specific heat data change. Therefore they cannot represent equilibrium values.

Every experimental technique used to measure specific heat has a characteristic rate of temperature change which sets the kinetics of the transformation along the coexistence interval during the measurement. This kinetics impact the results which explain the myriad of different specific heat peaks obtained from different techniques[18-20,22]

The new method was then tested on the M transition. A train of N=4 pulses was set with the first pulse (A) producing a temperature increment in the sample of 0.22 K ($W=3.85\text{mW}$, $Q=2.80\text{J}$) and the remaining three pulses (B) being 25 times smaller ($W=0.15\text{mW}$, $Q=0.11\text{J}$, $\Delta T=0.01\text{K}$). The scanning temperature rate for this experiment was 0.04 K/h.

Figure 4 shows the results under these conditions. Only around the M transition results for the new method markedly differ from results for the standard method, as we had predicted.

For A pulses the sample is markedly heated during the dissipation branch which, after some temperature is reached, makes the transformation begins. The associated enthalpy modifies the transient response by the fluxmeter and prevents from reaching a stationary state at the prescribed time τ (the intermittent behaviour of the transformation characteristically induces heat peaks during the dissipation branch. The thermal signature of these jerks extends to the relaxation branch). Dissipation and relaxation specific heats c_d and c_r show a peak which is larger in amplitude and width for c_d .

Thermal hysteresis is expected to prevent the reversal transformation after the sample relaxes from pulse A. Notice that NiMnIn compounds typically show hysteresis larger than 1K in the M transformation. Ideally during a B pulse the dissipation branch should not be able to bring new transformations in the sample. Our experimental results fit to this hypothesis: the peak disappears for pulse B data while c_d and c_r match to each other within our experimental resolution.

Figure 4b shows ΔH_i (see Equation 6) versus temperature. For the FP phase transition, ΔH_i is zero for all the pulses, irrespective of their amplitude. This is the signature of a second order phase transition.

For the M transition, ΔH_i is markedly different from zero for A pulses. For B pulses, ΔH_i is about 0.4% of ΔH_i for A pulses (see the inset in panel (b)). The magnitude of the anomaly decreases for pulses B₂ and B₃. It indicates that although there is still a remnant phase transition taking place, the involved fraction of sample is much smaller.

Although the sensitivity of the system allows to measure such small enthalpy changes during B pulses, they are not large enough to significantly modify the specific heat results. While for A pulses ΔH_i is 9% of Q at most, for B pulse it only amounts to 0.4% of Q at most, which is unable to exclude a null c_d - c_r within our experimental resolution.

The anomaly for c_p then looks like a one-step transition between the value corresponding to either phase. The signature is similar to that obtained in a sample of the same family but without the peak in the specific heat that is observed in Ref. [18]. The difference between the specific heat for both phases could be related to the different magnetic character of both phases. Measurements of the magnetization would be necessary to ascertain the origin of the difference but this study is beyond the scope of this paper.

ΔH_i is non-zero from 280K and 295K. The enthalpy jump associated to the M transition is obtained by adding up ΔH_i for each cycle, giving $\Delta H=7.06$ J/g or 468 J/mol. The value of the enthalpy of transition agrees with the reported values for the martensitic transformation in $\text{Ni}_{0.50}\text{Mn}_{0.50-x}\text{In}_x$ [28].

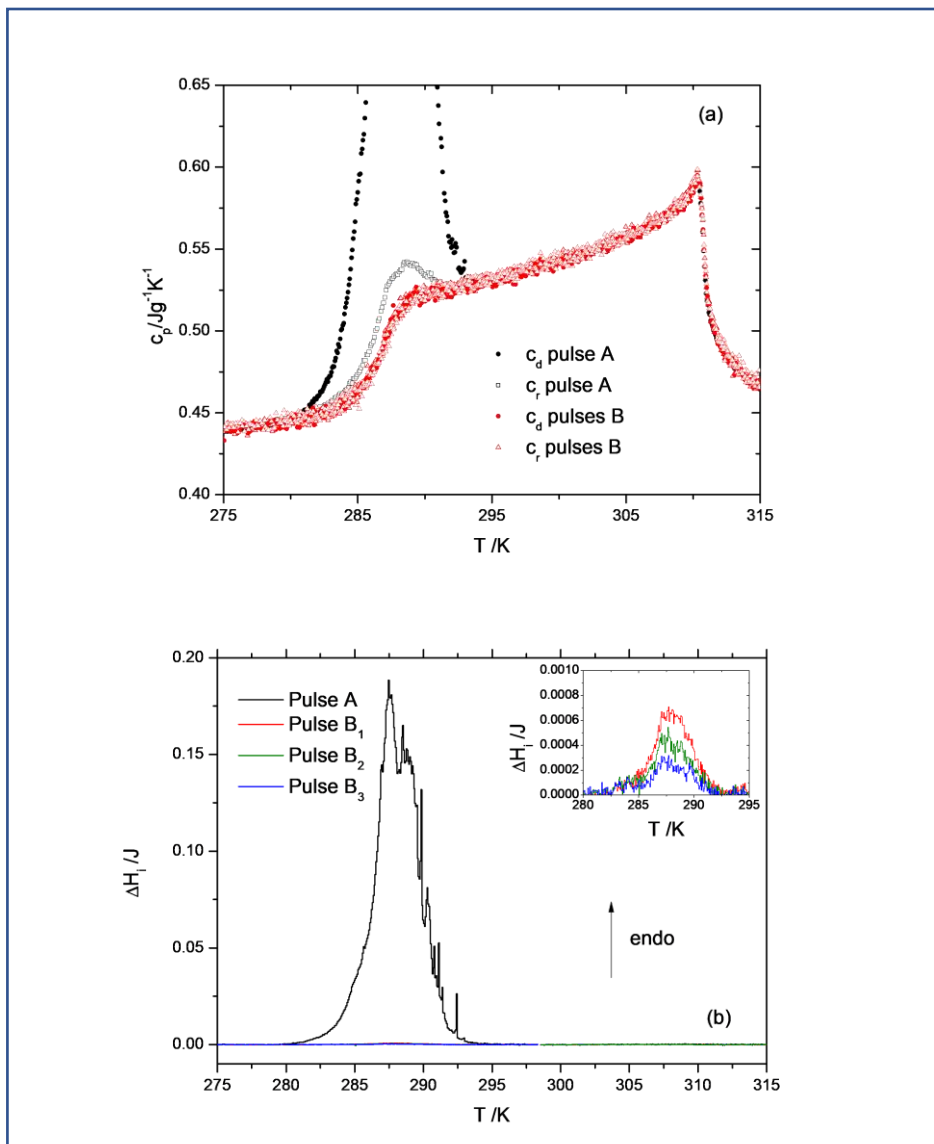


Figure 4: (a) Specific heat data vs temperature in a $\text{Ni}_{50.54}\text{Mn}_{33.65}\text{In}_{15.82}$ sample. Specific heat were obtained from a train of amplitude modulated train of heat pulses through Eq. 4 and 5, (b) the transition enthalpy vs temperature in the same run obtained from Eq. 6. The inset in panel (b) enlarges the coexistence interval for pulses B.

5. CONCLUSIONS

A new technique able to discriminate transition enthalpy (energy stored structurally) from specific heat (energy stored kinetically) in first-order structural phase transitions has been designed and successfully tested on a sample of $\text{Ni}_{50.54}\text{Mn}_{33.65}\text{In}_{15.82}$.

The technique uses amplitude-modulated heat pulses during heating scans. The amplitude of one in every four pulses is exceedingly large ($\Delta T \sim 0.2\text{K}$) so as to induce phase transformation which stores energy structurally and gives rise to transition enthalpy. In the remaining pulses the amplitude is decreased by a factor 25 so that phase transformation is inhibited due to hysteresis and the specific heat for the given molar fraction of phases can be determined.

For the $\text{Ni}_{50.54}\text{Mn}_{33.65}\text{In}_{15.82}$ phase transitions results show that the ferromagnetic-paramagnetic transition is continuous while the martensitic phase transition is discontinuous. In the latter, the specific heat smoothly changes during the coexistence interval from the austenite value to the martensite value.

The amplitude modulated design of heat pulses could be also applied to other calorimetric techniques which take advantage of heat pulses to measure specific heat.

A bold challenge is to adapt the amplitude modulation to cooling scans. This would require to replace the heaters by a Peltier or a thermomagnetic device because in cooling scans phase transformation requires further active cooling.

6. ACKNOWLEDGMENTS

The authors wish to thank Prof. A. Planes (Universidad de Barcelona) for supplying the sample and Dr. R. Cano (Universidad de Sevilla) for his help in cutting the sample.

BIBLIOGRAPHY

- [1] B. Wunderlich, *Thermal Analysis*, Academic Press, 1990.
<https://doi.org/https://doi.org/10.1016/B978-0-12-765605-2.50005-4>.
- [2] M.W. Zemansky, *Heat and thermodynamics; an intermediate textbook*, Fifth edition. New York : McGraw-Hill, [1968], n.d.
<https://search.library.wisc.edu/catalog/999473407602121>.
- [3] E.S.R. Gopal, *Specific heats at low temperatures*, Springer US, 1966.
<https://doi.org/10.1007/978-1-4684-9081-7>.
- [4] P.F. Sullivan, G. Seidel, Steady-State, ac-Temperature Calorimetry, *Physical Review*. 173 (1968) 679–685. <https://doi.org/10.1103/PhysRev.173.679>.
- [5] R. Bachmann, F.J. DiSalvo, T.H. Geballe, R.L. Greene, R.E. Howard, C.N. King, H.C. Kirsch, K.N. Lee, R.E. Schwall, H. -U. Thomas, R.B. Zubeck, Heat Capacity Measurements on Small Samples at Low Temperatures, *Review of Scientific Instruments*. 43 (1972) 205–214. <https://doi.org/10.1063/1.1685596>.
- [6] J. del Cerro, New measurement method of thermal properties by means of flux calorimetry, *Journal of Physics E: Scientific Instruments*. 20 (1987) 609–611.
<https://doi.org/10.1088/0022-3735/20/6/005>.

- [7] H. Suzuki, A. Inaba, C. Meingast, Accurate heat capacity data at phase transitions from relaxation calorimetry, *Cryogenics*. 50 (2010) 693–699. <https://doi.org/https://doi.org/10.1016/j.cryogenics.2010.07.003>.
- [8] V. Hardy, Y. Bréard, C. Martin, Derivation of the heat capacity anomaly at a first-order transition by using a semi-adiabatic relaxation technique, *Journal of Physics: Condensed Matter*. 21 (2009) 75403. <https://doi.org/10.1088/0953-8984/21/7/075403>.
- [9] J.C. Lashley, M.F. Hundley, A. Migliori, J.L. Sarrao, P.G. Pagliuso, T.W. Darling, M. Jaime, J.C. Cooley, W.L. Hults, L. Morales, D.J. Thoma, J.L. Smith, J. Boerio-Goates, B.F. Woodfield, G.R. Stewart, R.A. Fisher, N.E. Phillips, Critical examination of heat capacity measurements made on a quantum design physical property measurement system, *Cryogenics*. 43 (2003) 369–378. [https://doi.org/10.1016/S0011-2275\(03\)00092-4](https://doi.org/10.1016/S0011-2275(03)00092-4).
- [10] V.K. Pecharsky, K.A. Gschneidner, Heat capacity near first order phase transitions and the magnetocaloric effect: An analysis of the errors, and a case study of Gd₅(Si₂Ge₂) and Dy, *Journal of Applied Physics*. 86 (1999) 6315–6321. <https://doi.org/10.1063/1.371734>.
- [11] F. Guillou, A.K. Pathak, D. Paudyal, Y. Mudryk, F. Wilhelm, A. Rogalev, V.K. Pecharsky, Non-hysteretic first-order phase transition with large latent heat and giant low-field magnetocaloric effect, *Nature Communications*. 9 (2018). <https://doi.org/10.1038/s41467-018-05268-4>.
- [12] J. del Cerro, J.M. Martín-Olalla, F.J. Romero, Square modulated differential thermal analysis, *Thermochimica Acta*. 401 (2003) 149–158. [https://doi.org/DOI:10.1016/S0040-6031\(02\)00545-2](https://doi.org/DOI:10.1016/S0040-6031(02)00545-2).
- [13] J. del Cerro, J. Manchado, F.J. Romero, M.C. Gallardo, Square-modulated differential thermal analysis: measuring method, *Measurement Science and Technology*. 23 (2012) 35003. <https://doi.org/10.1088/0957-0233/23/3/035003>.
- [14] V.K. Sharma, M.K. Chattopadhyay, R. Kumar, T. Ganguli, P. Tiwari, S.B. Roy, Magnetocaloric effect in Heusler alloys Ni₅₀Mn₃₄In₁₆ and Ni₅₀Mn₃₄Sn₁₆, *Journal of Physics Condensed Matter*. 19 (2007) 0–12. <https://doi.org/10.1088/0953-8984/19/49/496207>.
- [15] M.C. Gallardo, J. Jiménez, J. del Cerro, Experimental device for measuring the influence of a uniaxial stress on specific heat: Application to the strontium titanate ferroelastic crystal, *Review of Scientific Instruments*. 66 (1995) 5288–5291. <https://doi.org/10.1063/1.1146100>.
- [16] F.J. Romero, M.C. Gallardo, A. Czarnecka, M. Koralewski, J. del Cerro, Thermal and kinetic study of the ferroelectric phase transition in deuterated triglycine selenate, *Journal of Thermal Analysis and Calorimetry*. 87 (2007) 355–361. <https://doi.org/10.1007/s10973-005-7444-7>.
- [17] X. Moya, L. Mañosa, A. Planes, S. Aksoy, M. Acet, E.F. Wassermann, T. Krenke, Cooling and heating by adiabatic magnetization in the Ni₅₀ Mn₃₄ In₁₆ magnetic shape-memory alloy, *Physical Review B - Condensed Matter and Materials Physics*. 75 (2007) 1–5. <https://doi.org/10.1103/PhysRevB.75.184412>.

- [18] A.B. Batdalov, A.M. Aliev, L.N. Khanov, V.D. Buchel'nikov, V. v. Sokolovskii, V. v. Koledov, V.G. Shavrov, A. v. Mashirov, E.T. Dil'mieva, Magnetic, thermal, and electrical properties of an Ni_{45.37}Mn_{40.91}In_{13.72} Heusler alloy, *Journal of Experimental and Theoretical Physics*. 122 (2016) 874–882. <https://doi.org/10.1134/S1063776116040129>.
- [19] M.K. Chattopadhyay, M.A. Manekar, V.K. Sharma, P. Arora, P. Tiwari, M.K. Tiwari, S.B. Roy, Contrasting magnetic behavior of Ni₅₀Mn₃₅In₁₅ and Ni₅₀Mn_{34.5}In_{15.5} alloys, *Journal of Applied Physics*. 108 (2010). <https://doi.org/10.1063/1.3478774>.
- [20] J.H. Chen, N.M. Bruno, I. Karaman, Y. Huang, J. Li, J.H. Ross, Calorimetric and magnetic study for Ni₅₀Mn₃₆In₁₄ and relative cooling power in paramagnetic inverse magnetocaloric systems, *Journal of Applied Physics*. 116 (2014) 1–8. <https://doi.org/10.1063/1.4902527>.
- [21] A.N. Vasiliev, O. Heczko, O.S. Volkova, T.N. Vasilchikova, T.N. Voloshok, K. v. Klimov, W. Ito, R. Kainuma, K. Ishida, K. Oikawa, S. Fähler, On the electronic origin of the inverse magnetocaloric effect in Ni-Co-Mn-In Heusler alloys, *Journal of Physics D: Applied Physics*. 43 (2010). <https://doi.org/10.1088/0022-3727/43/5/055004>.
- [22] S.M. Podgornykh, E.G. Gerasimov, N. v. Mushnikov, T. Kanomata, Heat capacity of the Ni₅₀Mn₃₇(In_{0.2}Sn_{0.8})₁₃ alloy, *Journal of Physics: Conference Series*. 266 (2011) 0–5. <https://doi.org/10.1088/1742-6596/266/1/012004>.
- [23] M.C. Gallardo, J. Manchado, F.J. Romero, J. del Cerro, E.K.H. Salje, A. Planes, E. Vives, R. Romero, M. Stipcich, Avalanche criticality in the martensitic transition of Cu_{67.64}Zn_{16.71}Al_{15.65} shape-memory alloy: A calorimetric and acoustic emission study, *Physical Review B - Condensed Matter and Materials Physics*. 81 (2010) 1–8. <https://doi.org/10.1103/PhysRevB.81.174102>.
- [24] F.J. Romero, J. Manchado, J.M. Martín-Olalla, M.C. Gallardo, E.K.H. Salje, Dynamic heat flux experiments in Cu_{67.64}Zn_{16.71}Al_{15.65}: Separating the time scales of fast and ultra-slow kinetic processes in martensitic transformations, *Applied Physics Letters*. 99 (2011) 11906. <https://doi.org/10.1063/1.3609239>.
- [25] J. Baró, J.-M. Martín-Olalla, F.J. Romero, M.C. Gallardo, E.K.H. Salje, E. Vives, A. Planes, Avalanche correlations in the martensitic transition of a Cu–Zn–Al shape memory alloy: analysis of acoustic emission and calorimetry, *Journal of Physics: Condensed Matter*. 26 (2014) 125401. <https://doi.org/10.1088/0953-8984/26/12/125401>.
- [26] F.J. Romero, J.M. Martín-Olalla, M.C. Gallardo, D. Soto-Parra, E.K.H. Salje, E. Vives, A. Planes, Scale-invariant avalanche dynamics in the temperature-driven martensitic transition of a Cu-Al-Be single crystal, *Physical Review B*. 99 (2019) 1–7. <https://doi.org/10.1103/PhysRevB.99.224101>.
- [27] E. Vives, J. Baró, M.C. Gallardo, J.M. Martín-Olalla, F.J. Romero, S.L. Driver, M.A. Carpenter, E.K.H. Salje, M. Stipcich, R. Romero, A. Planes, Avalanche criticalities and elastic and calorimetric anomalies of the transition from cubic Cu-Al-Ni to a mixture of 18R and 2H structures, *Physical Review B*. 94 (2016) 1–8. <https://doi.org/10.1103/PhysRevB.94.024102>.

- [28] T. Krenke, M. Acet, E.F. Wassermann, X. Moya, L. Mañosa, A. Planes, Ferromagnetism in the austenitic and martensitic states of Ni-Mn-In alloys, *Physical Review B - Condensed Matter and Materials Physics*. 73 (2006) 1–10.
<https://doi.org/10.1103/PhysRevB.73.174413>.